Proceedings of the 2012 IEEE
International Conference on Robotics and Biomimetics
December 11-14, 2012, Guangzhou, China

Compliance Estimation during Bilateral Teleoperation of a Robotic Arm

Remo Pillat and Arjun Nagendran

Abstract— **A method for estimating compliance properties of objects in the workspace of remotely located robotic manipulators is presented herein. An architecture that supports decoupled remote teleoperation is briefly described, and used to control the manipulator during recovery of an object's compliance parameters. These parameters are based on the Kelvin-Voigt contact model and estimated in simulation as well as experimentally using offline and online estimation techniques. A comparison of the estimation techniques reveals that the proposed RANSAC-based technique is better suited to compliance recovery over existing methods, even in the presence of sensor noise. The recovered parameters are used to update a reconfigurable compliance object in simulation to closely match that of the real-world object, thereby enabling the use of realistic haptic feedback during remote teleoperation.**

I. INTRODUCTION

The field of haptics encompasses a broad swath of applications employing force-reflective user interfaces. In areas such as minimally invasive surgery, remote teleoperation, and robotic object manipulation, realistic haptic feedback can assist the operator in successful completion of a given task.

Haptic feedback in remote teleoperation environments is complicated by the permanent influence of transmission latencies and communication bandwidth limitations between the master controller and the slave executor [1]. This not only limits the abilities for direct control of the slave, but it also complicates the task of force reflection. To circumvent this problem, a different paradigm for bilateral teleoperation that uses a virtual reality simulation environment has been proposed recently [2]. It decouples the master and slave sides by letting the user execute the desired actions in the simulation environment and then transfers the operator's intent to a semi-autonomous slave instance that executes the movements.

To receive haptic feedback within this architecture, it is required to estimate the compliance properties of objects that are in the real robot's interaction space. These compliance parameters can then be used to update those of the object in the simulation environment (master), allowing haptic forces to be rendered such that they are reflective of the real world's mechanical properties.

The focus of this paper is the dynamic recovery of compliance properties of remote objects using the architecture described above. During the parameter estimation, the examined object is subject to controlled forces using an admittance scheme to avoid damaging interactions. While in contact, position, velocity, and force readings allow characterization of the object.

The main contributions of this manuscript are as follows. Two different offline methods for estimating the parameters of the Kelvin-Voigt [3] contact model have been developed, one of which uses RANSAC [4] to minimize noise sensitivity. To test these methods, data was gathered both in a comprehensive simulation as well as experimentally. The simulation encompasses closed loop force control of the manipulator, as well as a variable compliance object. A detailed analysis of algorithmic performance is performed for a range of compliance parameters. To evaluate the accuracy of the estimators in the presence of disturbances, a noise sensitivity analysis is performed and the results compared to the popular Self-Perturbing Recursive Least Squares (SPRLS) online estimation method. This analysis will provide guidance on the appropriate application cases of the evaluated methods.

The rest of the paper is organized as follows. Related literature on compliance estimation is reviewed in Section II. Section III presents a system architecture supporting teleoperation with force feedback and a hybrid control scheme for a serial-link robot arm is detailed in Section IV. Section V lays out different compliance parameter estimation procedures. Relevant experimental results (both simulation and real-world) are analyzed in Section VI and the paper is concluded in Section VII.

II. BACKGROUND

Since this paper focuses on the compliance estimation of unknown objects, this background section provides an overview of prior research in that area. For abstracting contact dynamics, commonly either the linear Kelvin-Voigt model [3] or the non-linear Hunt-Crossley model [5] are employed. In the Kelvin-Voigt model the relationship of penetration depth to encountered force is expressed by a parallel spring / dashpot system, whereas the Hunt-Crossley model extends this relationship to a non-linear one.

Generally, estimation algorithms for these models are based on one of two approaches: Recursive Least Squares (RLS) estimation and its variants or adaptive control methods. The authors of [6] use an RLS estimation for recovering stiffness and damping environment parameters for the Kelvin-Voigt model. RLS was also employed by [7] to estimate the non-linear parameters for the Hunt-Crossley model. In general, RLS is only able to reliably estimate linear models, but the authors circumvented that problem by using two interconnected RLS estimators linked via a crossed feedback loop. A different approach to linearization is elaborated in [8]. Using the natural logarithm and assuming

R. Pillat is with the Synthetic Reality Lab, University of Central Florida, Orlando FL, 32826, USA rpillat@cs.ucf.edu
A. Nagendran is with the Institute of Simulation and Training, University of Central Florida, Orlando FL, 32826, USA arjun@cs.ucf.edu

that penetration speed and sensor noise are small, the Hunt-Crossley model can be linearized in the parameters. These are subsequently recovered by the Exponentially Weighted Recursive Least Squares (EWRLS) algorithm. The authors show superior estimation performance compared to [7].

The authors of [9] use the same linearizing method, but employ a modified RLS method called Self-Perturbing Recursive Least Squares (SPRLS) to estimate the Kelvin-Voigt and Hunt-Crossley models in parallel. This hybrid approach shows very promising results and switches between the models based on the estimated environment stiffness. SPRLS is also employed for contact impedance estimation by [10] in the framework of a teleoperation scheme. The relative popularity of SPRLS in recent years can be explained by the fact that in a direct comparison between RLS, EWRLS, and SPRLS in [11], the latter was confirmed to be most resistant to noise disturbances. In Section VI-C, this noise-resistance claim will be tested against other methods described here.

Another family of compliance estimation methods are control-based approaches that tightly integrate the environment estimation component in an open- or closed-loop robot control system. In general, this control-centric approach simplifies the stability analysis of the resulting manipulation system.

Seraji et al developed a scheme for stiffness and damping estimation with an indirect adaptive control approach [12]. The authors show the performance improvement of a force-tracking impedance controller with the added online estimation component. [13] extends this work by evaluating the influence of persistent excitation on the parameter estimation and how haptic feedback of the excited signal can be avoided. [14] uses a model-reference adaptive control scheme to provide environment estimates and constant force tracking, but the paper limits the environment parameters to pure stiffness.

Good comparisons between the different estimation methods can be found in [15] and [16].

The focus of this paper will be on the development and analysis of algorithms for the estimation of Kelvin-Voigt parameters. Due to the popularity of RLS-based methods, the performance of one of its representatives in the presence of noise will be used for comparison.

III. ARCHITECTURE

Receiving direct haptic feedback while controlling a remote robot is impeded by inherent latency and bandwidth issues, which are characteristic of any teleoperation system. Figure 1 illustrates the architecture that uses a simulated virtual environment to decouple the master operator from the slave robot. This architecture relieves the complexities of implementing a direct control scheme in the presence of variable time delays and presents the user with better response time and system transparency. In essence, a human operator works in a virtual environment, consisting of a robotic arm and a re-configurable compliance object, to plan and execute a series of robot motions. Only specified target configurations are transmitted to the slave instance, which displays adaptability (semi-autonomy) in execution of these commands. While not the essence of this manuscript, a variation of this architecture is described in detail in [2] and is important for tasks that require remote manipulation that can be enhanced using haptic feedback.

The slave-instance uses one of the developed methods to estimate the properties of compliance objects at its end, and passes these values back to the master, which in turn updates the compliance properties of the object in the master-side virtual simulation. While this allows realistic force-feedback to be received via a Phantom Omni or similar device, the experiments in Section VI only focus on compliance estimation without transmitting these forces back to the user.

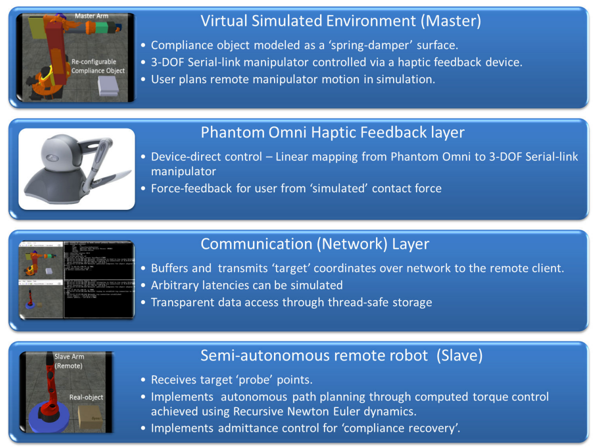

Fig. 1. Components of the decoupled haptic feedback architecture

IV. CONTROL

A serial-link remote robot arm (slave-side) was equipped with a single-axis force sensor at its end effector and actuated by DC motors. Torque sensors at the joints were used to measure the commanded control signal while rotary encoders were used for joint position feedback. Coordinate frames for the serial-link robotic arm are assigned using the Denavit-Hartenberg, or D-H convention.

A. DH Parameters and Kinematics

The slave side robot is required to probe the object in its space on receiving a position command from the master. The robotic arm attempts to maintain the exact orientation at which the end effector makes contact with the object on the master side. For the chosen 3-link serial manipulator, redundancy in the manipulator configuration allows us to compute the desired angles to achieve a target $[x_t\ y_t]^T$ using closed form inverse kinematics solutions.

B. Manipulator Dynamics

The Recursive Newton Euler (RNE) method was used to calculate the joint torques from the motion of the manipulators that make up the system, and included gravity compensation. In general, the torque on a joint i is calculated as

$$\tau_i = N_i + \tau_{i+1} +^i f_{i,y} C_i +^i f_{i+1,y}(L_i - C_i) \qquad (1)$$

where N_i is the moment of inertia of link i about its rotation axis, τ_i is the torque on the i^{th} link, ${}^i f_{i,y}$ is the y-component of the force exerted on link i by link $(i-1)$, ${}^i f_{i+1,y}$ is the y-component of the external force acting on link (i), C_i is the position of the centroid of link i from joint-frame i and L_i is the length of link i.

Serial link manipulators are notorious for their coupling effects that are more pronounced when the masses of the links that make up the system are significant. A computed torque controller with a secondary PID controller for disturbance rejection was therefore implemented for accurate position control.

C. Manipulator Admittance

According to [17], contact tasks are those in which a robot grasps, pushes, or works against a work piece. There is a dynamic interaction between the manipulator and the object being probed, invoking a change in the response of the system to its actuator. Impedance Control attempts to implement a dynamic relationship between manipulator variables such as force and end point position, rather than controlling each of these variables alone [17]. This relationship can be described assuming spring-damper properties for the object being manipulated. i.e. $F_{act} = k(x_d - x_t) + c\frac{d}{dt}(x_d - x_t)$ where $x = x_d - x_t$ is the displacement of the end effector after contact with the object in its workspace. In admittance control, the response to a measured force is a change in position. To achieve this, an external position feedback control loop is implemented around the force controller as shown in Figure 2. A dynamic relationship between the end-effector actual and desired positions and forces is thus enforced.

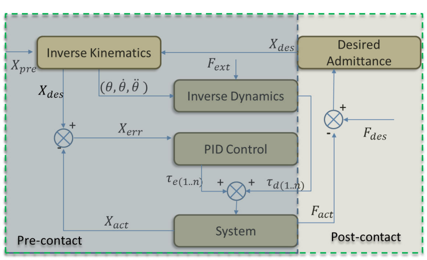

Fig. 2. The hybrid control system of admittance and computed torque control. Prior to contact, a position demand X_{pre} is passed to the inverse kinematic block. The output from the inverse dynamics controller and the secondary PID controller for disturbance rejection (from external forces F_{ext}) are summative and are output to the system. X_{des} is the same as X_{pre} during this stage. Once contact is established, the error between the desired force F_{des} and F_{act} is passed through the admittance block. This results in a new desired position X_{des} in response to the force. τ is the computed torque for the system and $[\theta, \dot{\theta}, \ddot{\theta}]$ are the angular position, velocity and accelerations required to achieve the desired path.

The controller is hybrid in nature, transitioning between non-contact and contact states in a fast and stable manner, as required for a task such as compliance estimation. The desired admittance control law outputs a change in position in response to a force, prior to which the computed torque controller is used for path planning as shown in Figure 2.

V. PARAMETER ESTIMATION

Object compliance estimation in haptic teleoperation scenarios helps provide the user with an adequate level of transparency. Though the architecture presented in Section III alleviates the direct control problem by decoupling the master and slave instances through a simulation layer, the question of how haptic feedback can be treated in such a scenario remains.

To ease the estimation process, it is assumed that the probed material can be approximated by a parallel spring-damper system (see Section IV-C), also sometimes referred to as Kelvin-Voigt contact model [3]. In this case, the spring constant k and the viscous damping coefficient c fully describe a linear relationship between penetration depth x of the end effector, its velocity $\dot{x}$ and the encountered force F: $F = kx + c\dot{x}$.

To estimate k and c, it is assumed that data points of end effector position, velocity, and contact forces can be gathered at fixed time intervals. The end effector position can be either directly measured through external tracking or derived through forward kinematics; its probing velocity can be found either by position differentiation or direct measurement. Contact forces are measured by a force sensor mounted on the end effector.

After the master operator defines a set of probing points, the slave executes the probing action semi-autonomously. Once contact with the surface has been established, the admittance controller ensures that a controlled force is exerted on the object, without damaging it. Since the damping coefficient c can only be estimated through varying end effector velocity, the same probing motion will be executed at multiple velocities.

With the gathered sample points, the following linear relationship can be established:

$$\mathbf{F} = \mathbf{A} \begin{bmatrix} k & c \end{bmatrix}^T \qquad (2)$$

It is assumed that there are n samples of the end effector displacement x, its velocity $\dot{x}$ and measured force F_{act}. Then $\mathbf{F}$ is a $(n\text{x}1)$ matrix of all force readings and $\mathbf{A}$ is a $(n\text{x}2)$ matrix of the measured displacements and velocities. The unknown values in this equation are the spring constant k and the viscous damping coefficient c.

If $n > 2$, this system is over-defined and an approximated solution has to be found. Commonly, a system like Equation (2) is solved in the least-squares sense by using the pseudo-inverse. This method will be referred to as LSQ in the rest of this paper and serves to establish a baseline performance.

In addition, a RANSAC [4] scheme has been implemented that provides greater robustness to sample outliers and rejects degenerate solutions. In the presence of noise, RANSAC effectively samples different subsets of the gathered data and evaluates a least squares fit for each subset. The recovered parameters are then tested against the whole data set and inliers and outliers are identified. Although RANSAC has been used extensively in a variety of application cases, to our knowledge this paper is the first to evaluate a RANSAC-based estimation method for object compliance.

Both LSQ and RANSAC are offline methods since they require a complete set of force, position, and velocity readings.

VI. RESULTS

Accuracy and noise resistance are paramount metrics in the evaluation of a compliance estimation algorithm. To validate the proposed methods in terms of these criteria, simulated as well as real experimental results were compared for LSQ, RANSAC, and Self Perturbing Recursive Least Squares (SPRLS), a popular online estimation method. The noise disturbance analysis in particular provides useful insights into the choice of an appropriate estimation algorithm.

In addition, the effectiveness of the computed torque controller on the slave robot was evaluated.

A. Controller Performance in Simulation

The measured torques from sensors mounted at the joints were compared to the commanded joint torques during the execution of the contact task on the slave side. Figure 3a reveals that the measured torque follows the commanded torque very closely. This verifies the inverse dynamics model used during the experiment, which is significant since the approach is model-based, with errors propagating through the system resulting in instability. Additionally, torque at the first joint is much higher than that of the second joint, which is as expected due to the inertial loading of the serial manipulator.

Figure 3b shows the transition between non-contact and contact states when the end effector encounters the compliance object. The control scheme exhibits minimal spikes in the control torque on all the joints, thereby ensuring its stability. A constantly increasing magnitude in torque is noticed on all joints due to the increase in end effector force as the compliance object is compressed.

B. Parameter Estimation in Simulation

Both master and slave instances are represented by a virtual 3 DOF robot arm in simulation. The slave arm has a different kinematic configuration than the master arm to demonstrate the master-slave decoupling. An object of unknown spring-damper properties is part of the simulated scene and is probed by the arm. Once a target point on the object surface is specified by the user, it is transmitted to the slave, which executes the necessary movements to achieve this target.

The end effector on the simulated slave robot arm is lowered to the object surface at three different velocities (150 mm/s, 90 mm/s and 60 mm/s). Data points are gathered and stored at regular intervals from point of contact until a maximum end effector force of 10 N is achieved. A typical set of force vs. displacement readings for one of these tests is shown in Figure 4a. Even though this data is gathered in a simulated environment, it is far from noise-free and provides good test cases for the estimation algorithms.

In the virtual simulation environment, the spring constant k and the viscous damping coefficient c of the test object are varied. Each permutation of k and c is tested 3 times and the achieved results are averaged. The absolute difference of the resulting estimate and the ground truth value is our measure of performance and will be denoted simply as mean error.

Two offline methods are used to estimate these parameters: Least-Squares (LSQ) and RANSAC. The LSQ method has no free parameters. For RANSAC, the inlier threshold is chosen as 0.01 and a minimum number of 5 samples is required for a complete subset.

Results of estimating c for different spring constants are shown in Figure 4c. Figure 4b shows a similar plot for estimating k for varying damping coefficients. Overall, RANSAC provides a significant advantage over the simpler LSQ solution, particularly for spring-damper systems where the damping coefficient c is significantly greater than 0.

In all RANSAC test cases, k is recovered to within about 6.5% of its ground truth value and c within about 18.4% of its real magnitude, whereas the comparable numbers for LSQ are 20.6% and 29.5%.

C. Parameter Estimation under Simulated Noise

In any realistic scenario involving a physical slave robot arm, noise disturbances of the sensor signals are expected. In particular, force sensors are well known to routinely exhibit non-linear measurement behavior and are prone to noise disturbances. Any practical estimation of object properties needs to be sufficiently robust to tolerate these problems. Force measurements in simulation were therefore disturbed by Gaussian-distributed noise with zero mean and a standard deviation of $0 - 10\%$ of the force magnitude.

In addition to the previously discussed methods, this section also analyzes how noise affects the results of the popular SPRLS estimation method. SPRLS is an online estimation method that has gained popularity within the contact estimation community and achieved good results in [9], [10]. It is based on a Recursive Least Squares (RLS) estimator, but perturbs the process covariance matrix if the estimation error gets too small. According to [11] this process perturbation leads to superior process tracking and noise disturbance rejection compared to other RLS derivatives. The comparison of this online method against the presented offline methods is arguably lopsided, but provides useful insights into the upper limits of performance and estimation behavior in the presence of noise. SPRLS has multiple free parameters that need to be tuned for a specific noise environment. In the following tests, these parameters were optimized for an average noise case and then kept constant for all other test runs. Following the notation in [9], the design constant is chosen as $\beta = 20$ and the sensitivity gain is set to $\gamma = 1$. SPRLS was run online for every sample point, but only the last estimate was used for the algorithmic comparison.

Figure 4d shows the mean error of the estimates for k and c. Interestingly, the performance of LSQ as well as the

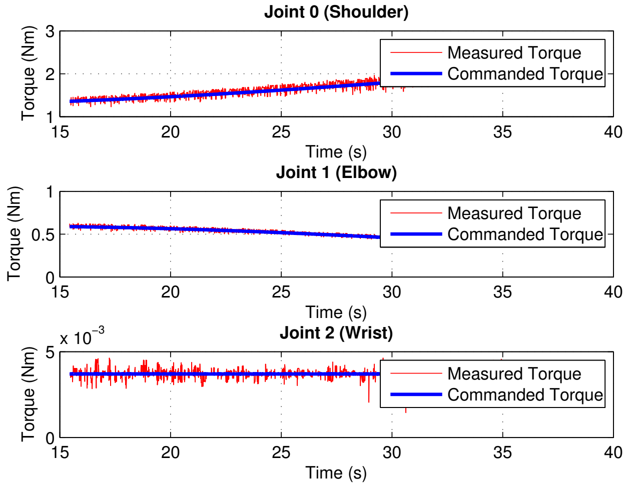

(a) The actual and commanded joint torques for each of the three joints of the 3-link serial robotic arm

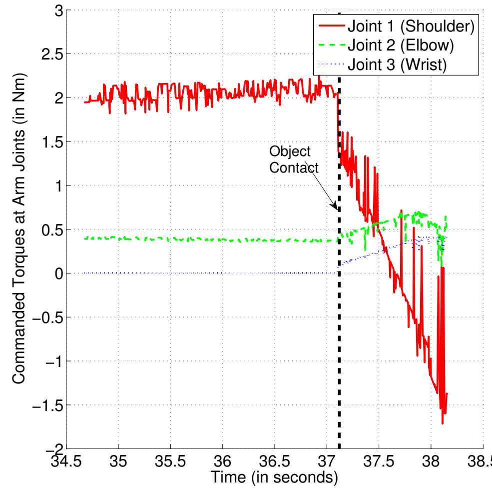

(b) Plot of torque between non-contact and contact states (against time)

Fig. 3. Controller performance - Measured and Commanded Torques

RANSAC estimation deteriorates, but both estimates stay within a reasonable band around the ground truth of $k = 500$ and $c = 100$. RANSAC does provide better noise rejection behavior, especially at higher noise magnitudes. SPRLS is the worst-performing algorithm and shows considerable divergence from the true value.

The good performance of RANSAC confirms the observations in Section VI-B, but the inferior results of SPRLS need to be explained. It seems that the perturbation term is the algorithm's weak point when noise tolerance is important. Initially introduced to allow the filter to react more rapidly to setpoint changes, the perturbations also make it more susceptible to noise in the input data. As noted by [11], the correct parameters for the SPRLS method are dependent on the actual material and noise characteristics, thus requiring careful tuning for each application instance. To confirm this, a separate test was executed with both β and γ being set to 0. In this case, the performance of SPRLS is comparable to the LSQ results. If SPRLS is employed as estimation method, these results advise caution in the choice of parameters, depending on the expected noise environment.

It should be noted that the presented RANSAC method has a limited number of parameters that are held constant across all experiments in this paper. No case-specific adjustments are necessary. Additionally, the remote compliance recovery architecture presented herein is unaffected by the choice of online/offline estimation method. This is because the master can potentially receive an update after compliance properties are confirmed. Tasks can now be executed on the master-side, which a better reflection of the real world.

D. Parameter Estimation in Experiments

To test the presented methods on realistic objects, two cubes of silicone rubber were molded. Through the use of different molding compounds, the cubes differ in their inherent compliance and will be denoted as Cube A and Cube B (see photo in Figure 5). The manufacturer of the rubber provides detailed specifications on its mechanical properties, among them a value for the material's Young's (elastic) modulus E. Within the elastic range of stresses, an approximate value for the effective spring constant k can be calculated as follows:

TABLE I

MECHANICAL PROPERTIES OF SILICONE RUBBER CUBES. THE SPRING CONSTANT k IS ESTIMATED ACCORDING TO EQUATION (3).

Property	Cube A	Cube B
Width (mm)	75	75
Height (mm)	75	75
Depth (mm)	34	73
Young's Modulus E (N/mm^2)	0.24	0.76
Approx. Spring Constant k (N/m)	4812.78	7098.3

$$k = \frac{EA_0}{l_0} \tag{3}$$

Here E denotes the Young's (elastic) modulus of the used cube, A_0 is the area through which the force is applied, and l_0 is the original length of the object along the force axis. In the case of Cubes A and B, l_0 is their respective depth, while A_0 is approximated by the circular area being affected by the end effector indentation. This calculation yields an approximate value for the cubes' spring constant, but unfortunately there is no equivalent approximation for their damping coefficients. It should be noted that these values only provide rough guidance and do not constitute ground truths, because individual material defects, the force area approximation, and the neglect of damping properties will lead to inaccuracies. The mechanical properties of the cubes are summarized in Table I.

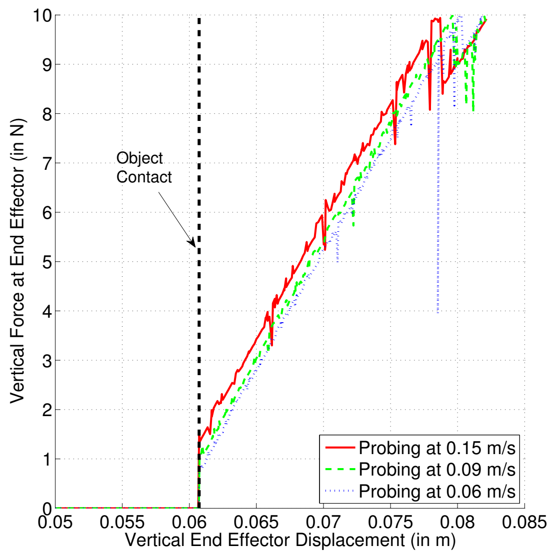

(a) Encountered end effector force during three approaches at different speeds. The simulated spring-damper constants are $k = 500$ and $c = 100$.

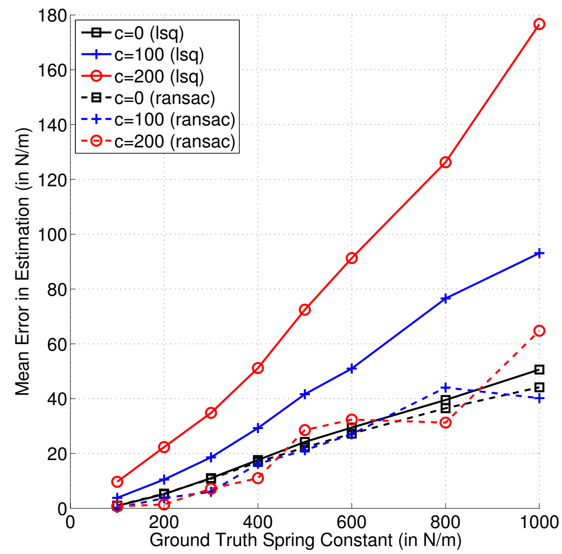

(b) Mean estimation errors of k.

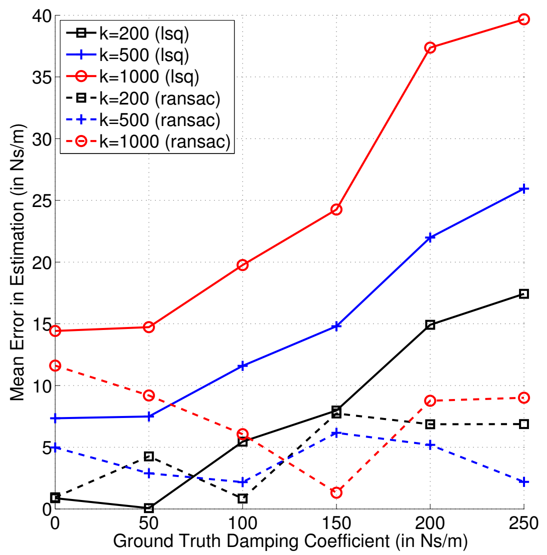

(c) Mean estimation errors of c.

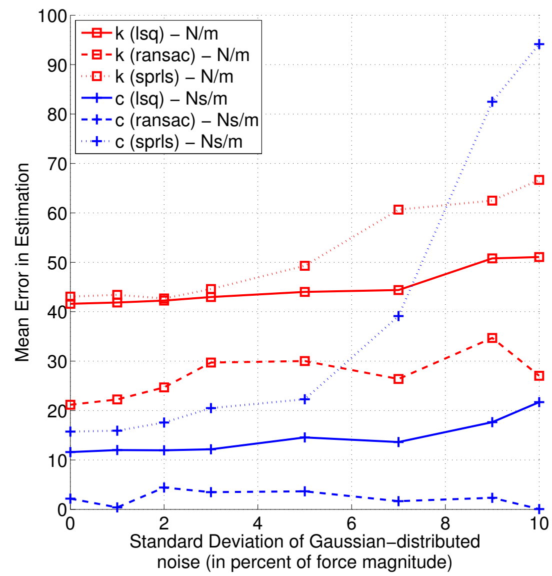

(d) Mean estimation errors under force sensor noise. Ground truth spring-damper constants are $k = 500$ and $c = 100$.

Fig. 4. Parameter estimation results for different spring constants k and viscous damping coefficients c.

As in the simulation, the object is probed three times at different velocities of 10, 20, and 50 mm/s. A uniaxial force sensor is mounted on the end effector and is used to directly record triplets of displacement, velocity, and encountered force data. The input parameters for the estimation methods are the same as in Section VI-B and VI-C.

Table II contains the estimated k and c values for the three different algorithms. The retrieved spring constant k lies in the expected value range (within 5%) returned by Equation (3), with all three methods returning very similar results. The estimates for the damping coefficient c differ considerably between the methods, ranging from almost 0 to over 300, but without further investigation it is hard to determine its true value.

Using results from both simulations and real experiments, it has been shown that all three estimation methods can successfully extract the spring and damping components of the Kelvin-Voigt model. In terms of robustness against noise, RANSAC exhibits superior performance compared to LSQ and the online SPRLS method. This suggests that if the

TABLE II

ESTIMATION RESULTS FOR SILICONE RUBBER CUBES FOR THE LINEAR LEAST-SQUARES (LSQ), RANSAC (RS), AND SELF-PERTURBING RECURSIVE LEAST-SQUARES (SPR) METHODS, RESPECTIVELY.

Cube	k (lsq)	k (rs)	k (spr)	c (lsq)	c (rs)	c (spr)
A	5021.53	4939.1	5034.99	115.11	313.81	74.25
B	7424.5	7311.2	7259.26	84.02	119.2	4.39

application allows the use of an offline method, a RANSAC-based estimator should be employed.

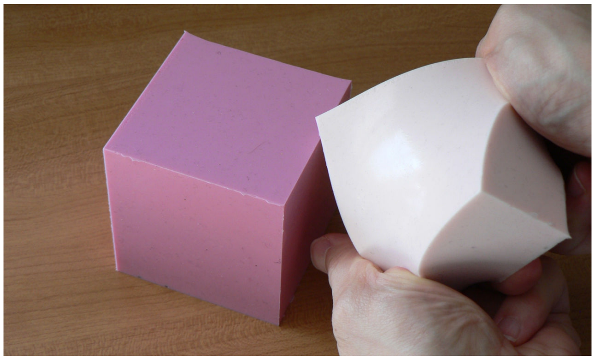

Fig. 5. A photo of the silicone cubes used in the experiments in Section VI-D.

VII. CONCLUSION

In this paper, methods were presented that allow the recovery of Kelvin-Voigt parameters through probing of a compliant object. Both offline LSQ and RANSAC algorithms were shown to reliably estimate these compliance properties, but RANSAC showed superior performance through its ability to reliably exclude outliers in noisy measurement data.

In comparison, the widely used online SPRLS method was shown to be very sensitive to noisy measurements and required application-specific parameter tuning. This implies that there is still room for improvement of existing online estimation schemes, as they do not yet approach the noise rejection ability and estimation accuracy of the offline methods.

In this work, the estimation methods were integrated into a bigger system that uses a decoupled control paradigm to allow user simulation-generated force feedback from remote robotic manipulators. Semi-autonomous control of a remotely located robotic arm using an admittance control scheme allows users to recover compliance properties of any objects located in its workspace, while ensuring exact force control at the end effector. The above system implementation lends itself to the use of an offline RANSAC-based estimation for recovering compliance properties.

The superior performance of RANSAC warrants future investigation into versions of the algorithm that allow online, recursive execution. Incremental or preemptive RANSAC are existing online variants, but their performance needs to be evaluated for compliance estimation tasks. Furthermore, the influence of different RANSAC parameters on the estimation performance should be evaluated more thoroughly. Other future work will involve recovering compliance parameters for non-linear contact models, like Hunt-Crossley.

ACKNOWLEDGMENTS

This work was partially supported by funds obtained from the Simulation for Healthcare Education and Learning Laboratory (SHELL) grant, sponsored by the Institute of Simulation and Training. The authors would also like to acknowledge the continued support and mentoring provided by Dr. Charles E. Hughes.

REFERENCES

[1] M. Tavakoli, R. V. Patel, and M. Moallem, *Haptics for Teleoperated Surgical Robotic Systems*. World Scientific, 2008.

[2] R. Pillat, A. Nagendran, and C. E. Hughes, "A Control Paradigm for Decoupled Operation of Mobile Robots in Remote Environments," in *International Conference on Computer Graphics Theory and Applications (GRAPP)*, 2012, pp. 553–561.

[3] M. A. Meyers and K. K. Chawla, *Mechanical Behavior of Materials*, 2nd ed. Cambridge University Press, 2008.

[4] M. A. Fischler and R. C. Bolles, "Random sample consensus: a paradigm for model fitting with applications to image analysis and automated cartography," *Communications of the ACM*, vol. 24, no. 6, pp. 381–395, June 1981.

[5] G. Gilardi and I. Sharf, "Literature Survey of Contact Dynamics Modelling," *Mechanism and Machine Theory*, vol. 37, no. 10, pp. 1213–1239, Oct. 2002.

[6] L. J. Love and W. J. Book, "Environment Estimation for Enhanced Impedance Control," in *IEEE International Conference on Robotics and Automation (ICRA)*, 1995, pp. 1854–1859.

[7] N. Diolaiti, C. Melchiorri, and S. Stramigioli, "Contact Impedance Estimation for Robotic Systems," *IEEE Transactions on Robotics*, vol. 21, no. 5, pp. 925–935, Oct. 2005.

[8] A. Haddadi and K. Hashtrudi-Zaad, "A New Method for Online Parameter Estimation of Hunt-Crossley Environment Dynamic Models," in *IEEE/RSJ International Conference on Intelligent Robots and Systems (IROS)*. IEEE, 2008, pp. 981–986.

[9] A. Achhammer, C. Weber, A. Peer, and M. Buss, "Improvement of Model-Mediated Teleoperation using a New Hybrid Environment Estimation Technique," in *IEEE International Conference on Robotics and Automation (ICRA)*, 2010, pp. 5358–5363.

[10] F. Mobasser and K. Hashtrudi-Zaad, "Implementation of a Rate Mode Impedance Reflecting Teleoperation Controller on a Haptic Simulation System," in *International Conference on Robotics and Automation (ICRA)*, no. April, 2004, pp. 1974–1979.

[11] T. Hunt, "A Comparative Study of System Identification Techniques in the Presence of Parameter Variation, Noise, and Data Anomalies," in *Midwest Symposium on Circuits and Systems*, vol. 2, no. 0. IEEE, 1996, pp. 593–596.

[12] H. Seraji and R. Colbaugh, "Force Tracking in Impedance Control," *The International Journal of Robotics Research*, vol. 16, no. 1, pp. 97–117, Feb. 1997.

[13] S. Misra and A. M. Okamura, "Environment Parameter Estimation during Bilateral Telemanipulation," in *Symposium on Haptic Interfaces for Virtual Environment and Teleoperator Systems*, 2006, pp. 301–307.

[14] S. K. Singh and D. O. Popa, "An Analysis of Some Fundamental Problems in Adaptive Control of Force and Impedance Behavior: Theory and Experiments," *IEEE Transactions on Robotics and Automation*, vol. 11, no. 6, pp. 912–921, 1995.

[15] D. Erickson, M. Weber, and I. Sharf, "Contact Stiffness and Damping Estimation for Robotic Systems," *The International Journal of Robotics Research*, vol. 22, no. 1, pp. 41–57, Jan. 2003.

[16] T. Yamamoto, M. Bernhardt, A. Peer, M. Buss, and A. M. Okamura, "Techniques for Environment Parameter Estimation during Telemanipulation," in *International Conference on Biomedical Robotics and Biomechatronics (Biorob)*. IEEE, Oct. 2008, pp. 217–223.

[17] N. Hogan, "Impedance control: An Approach to Manipulation, Part I - Theory, Part II - Implementation, Part III - Applications," *Journal of Dynamic Systems Measurement and Control*, vol. 107, pp. 1–24, 1985.